Channeling and Blocking of Energetic Charged Particles in Crystals

Jens Ulrik Andersen*

Department of Physics and Astronomy, University of Aarhus
8000 Aarhus C, Denmark

Abstract

The development of channeling and blocking since the foundation of the field was laid by Jens Lindhard in his classical paper in 1965 is discussed, and the question is asked whether this theory has passed the test of time. Have important aspects of the theory been challenged? Where has the theory needed modification or extension? Are there still open questions to be solved? A basic theoretical issue is the applicability of classical mechanics in the description. Lindhard showed that for particles heavy compared with the electron classical orbital pictures may always be applied. However, for electrons and positrons there are strong quantal features like Bragg interference. The quantal description introduced by Lindhard and co-workers has been used as the basis for a comprehensive treatment of the channeling of MeV electrons and positrons and of channeling radiation. At very high energies, GeV and TeV, the motion becomes classical, due to the relativistic increase of the field seen by the particles in the reference frame following their longitudinal motion. Channeling radiation in this regime is still an active field of research. For channeling and blocking of ions, the concept of statistical equilibrium plays a central part in Lindhard's theory. The application of this concept has been confronted with two important challenges, the first based on computer simulations and the second on experiments on the transmission of heavy ions through thin crystals. In both cases the challenges have been met and new insight has been gained but there are still problems to be solved. The channeling and blocking of ions have found very many applications, and a few problems and opportunities worth pursuing are suggested.

* E-mail: jua@phys.au.dk

Contents

Figure 1. Jens Lindhard gesturing with his pipe; with Larry Howe and the author. ICACS, Hamilton 1979.

1. Introduction

Channeling was discovered a few years before I began my graduate studies at the University of Aarhus in 1964, and I was lucky to be supervised by one of the pioneers in the field, John Davies, who brought the field to Aarhus. The local interest was stimulated by many lively "Saturday meetings" where new experimental developments were analysed and discussed. Most important was the strong involvement of Jens Lindhard, who with an impressive intellectual effort provided a theoretical foundation of the field in his famous paper from 1965 (Lindhard 1965). Before publication the theory was presented in a series of lectures, and I still remember these as a thrilling experience. There had been earlier theoretical work on channeling, including both computer simulations and analytical theory, but Lindhard's theory far surpassed this earlier work in depth of analysis, in generality of concepts, and in breadth of coverage of the phenomena. Lindhard presented his theory at the first of a series of International Conferences on Atomic Collisions in Solids (ICACS) and later developments in channeling were usually reported at these meetings. Figure 1 shows Lindhard at ICACS in Hamilton, 1979, in a characteristic pose using his pipe to make a point.

This is a brief review of the development of channeling during the following about forty years, based very much on my personal experience. I shall emphasize developments which I have found of particular interest and mainly refer to work that I have been involved in and therefore know best. I shall try to give credit

where needed to pioneering efforts by other groups but many more would have deserved to be mentioned. A main theme will be the further development of the theory of channeling on the basis of Lindhard's original paper. Have some of the basic concepts been challenged? Where has the theory been extended and where are new developments needed?

After the introduction of the basic concepts of channeling, the continuum potential and the continuum model, the question of quantum *versus* classical mechanics is considered. The quantum world of electron channeling and channeling radiation was for many years at the centre of my own interest. This is an aspect of channeling which was hardly touched upon in Lindhard's paper from 1965. However, shortly afterwards he published a paper on the quantum theory of channeling (Lervig et al., 1967), and I shall briefly discuss how this paper has provided a basis for a comprehensive, quantitative description of channeling radiation from MeV electrons and positrons. The physics of electron channeling at very high energies (GeV or TeV) is an active area of its own.

For ion channeling the focus will be on a key concept in Lindhard's theory. As a student I was especially impressed by the powerful applications of the concept of statistical equilibrium. Lindhard admired Gibbs' work on statistical mechanics and liked to quote Niels Bohr saying something like "this is how theory should be, at first very general and mathematical but then with great predictive power". Two attacks on the application of the hypothesis of statistical equilibrium in channeling will be discussed. They were based on computer simulations and on experiments, respectively. Because so fundamental concepts were challenged, the resolution of the problems has given important new insights.

The field of channeling covers an enormous area of experience and in this brief review it has been necessary to be selective. I have listed a few references to reviews covering in much more detail various aspects of channeling (Andersen et al., 1983a; Cohen and Dauvergne, 2004; Davies, 1983; Feldman et al., 1982; Gemmell, 1974; Gibson, 1975; Hofsäss, 1996; Krause and Datz, 1996; Sørensen and Uggerhøj, 1987, 1989; Uggerhøj, 2005). They may also be consulted for a more complete bibliography.

2. Collision with String of Atoms

When Lindhard first saw the picture in Figure 2 of an artist's perception of the passage of an ion through an open channel in a crystal lattice, his comment was: "this is not channeling!"

It is important to distinguish channeling from transparency. For channeling along a crystal axis, the motion is governed by correlated collisions with atoms

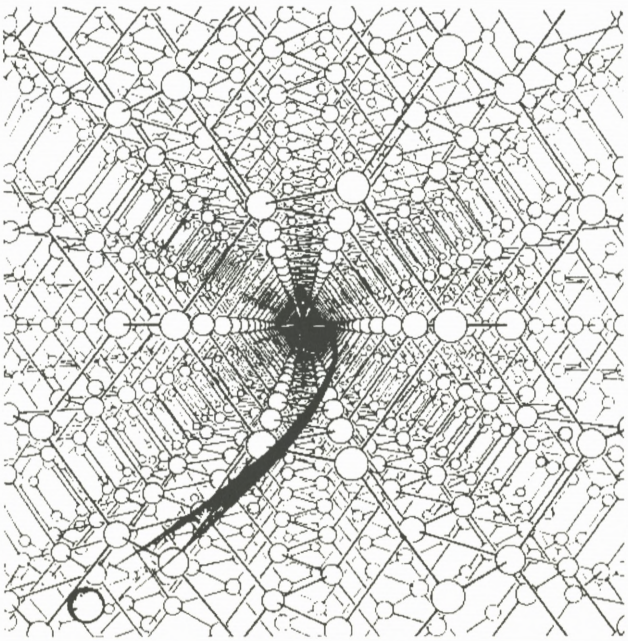

Figure 2. From "Channeling in Crystals" by W. Brandt, Sci. Am. 218, 91 (1968).

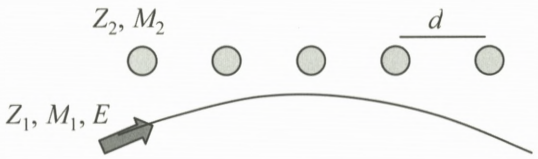

Figure 3. Deflection of ion by string of atoms.

aligned as pearls on a string, as illustrated in Figure 3. If many atoms contribute, the discrete deflections may be replaced by motion in the continuum string potential obtained by integration of the atomic interaction potential,

$$U(\vec{r}) = \frac{1}{d} \int dz V_{\text{at}}(\vec{r}, z). \tag{1}$$

Here z is the coordinate parallel to the string of atoms and $\vec{r} = (x, y)$ is the transverse coordinate vector. At large distances r, contributions from atoms on several strings must be included in the continuum potential.

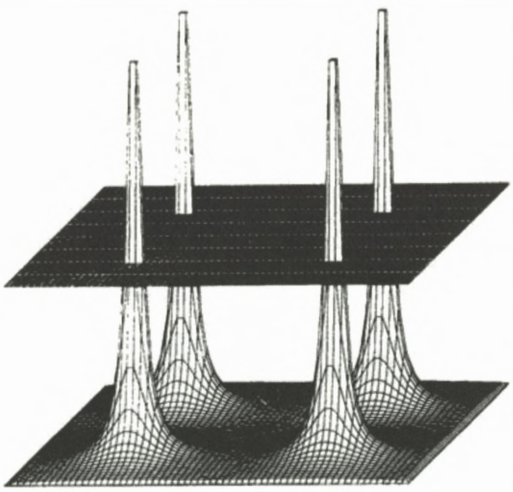

Figure 4. Axial continuum potential.

3. Continuum Model

In this continuum model there is a separation between the motion along the axis and the transverse motion, which is governed by a transverse Hamiltonian,

$$H(\vec{p}_\perp, \vec{r}) = \frac{p_\perp^2}{2M_1} + U(\vec{r}), \tag{2}$$

with conservation of transverse energy $E_\perp$. (For relativistic particles, $M_1 \to \gamma M_1$; Lervig et al., 1967.)

The string potential is repulsive and channeled ions are kept away from the atomic strings. The allowed area ($U(\vec{r}) < E_\perp$) within one unit cell in the transverse lattice of strings is denoted $A(E_\perp)$, and the total area per string is $A_0 = (Nd)^{-1}$ where N is the number density of the crystal. As illustrated in Figure 4, the motion is only for very low transverse energy confined to a single unit cell in the transverse lattice. In a classical *statistical equilibrium* at fixed $E_\perp$, with constant density on an energy shell in transverse phase space, the spatial density is constant in the allowed area for motion in two dimensions.

When the particle motion is restricted the particle is said to be channeled. Channeled particles do not have hard collisions with atoms and move through a gas of loosely bound atomic electrons. For particle incidence parallel to an axis there is therefore a very strong reduction in the yield of processes requiring a hard collision with an atom, like nuclear reactions or backscattering. Also energy loss and capture and loss of electrons are strongly modified.

4. Screened Potential

The Coulomb force between projectile and target nuclei is screened by electrons. A great simplification is obtained with Thomas–Fermi scaling:

$$U(r) = \frac{Z_1 Z_2 e^2}{d} \phi\left(\frac{r}{a}\right), \tag{3}$$

where $Z_1 e$ and $Z_2 e$ are the nuclear charges of projectile and atoms. The distance r is scaled with the Thomas–Fermi screening radius a, which for $Z_1 \ll Z_2$ is given in terms of the Bohr radius $a_0 = 0.53$ Å by

$$a = 0.8853 a_0 \, Z_2^{-1/3}. \tag{4}$$

A convenient approximation for analytical estimates is Lindhard's standard potential (Lindhard, 1965),

$$U(r) = \frac{Z_1 Z_2 e^2}{d} \ln\left(\frac{(Ca)^2}{r^2} + 1\right), \tag{5}$$

where $C \cong \sqrt{3}$. For distances r of order a, the potential is proportional to $1/r$, changing to $1/r^2$ at larger distances. Another commonly used and more accurate analytical approximation is the Molière potential. If the projectile charge is small and the screening is due only to the target electrons, a very accurate potential can be obtained from analytical approximations to the screened potential obtained from Hartree–Fock calculations (for example, the Doyle–Turner potential used often in calculations of electron diffraction and electron channeling; see Andersen et al., 1983a).

The question of the screening of the ion-atom potential is complex. It depends both on the atomic numbers of projectile and target and on the velocity of the projectile. According to the simple Bohr criterion, electrons bound to the ion with orbital velocities smaller than the ion velocity are stripped off. A characteristic velocity, separating between low velocities with nearly neutral projectiles and high velocities with only few electrons remaining on the ion, is therefore the Thomas–Fermi-scaled Bohr velocity, $Z_1^{2/3} v_0$.

The simplest case is for particles with $Z_1 \ll Z_2$ the limit of high velocities, where the screening radius, a, is determined by target electrons alone. If a few inner electrons with $\langle r \rangle \ll a$ remain on the projectile, giving it a net number of charges, Q, we may write the continuum potential $U^{(Q)}$ in terms of the potential $U^{(1)}$ for a proton as

$$U^{(Q)}(r) \cong Q U^{(1)}(r). \tag{6}$$

The number of charges, Q, can change by capture and loss but for well-channeled ions the cross sections are small and we may speak of "frozen charge states" for not too thick crystals (see Figure 28 below).

In the opposite limit of high Z_1 and low velocities the ion carries many electrons, is nearly neutral, and the screening is due to electrons on both target and projectile atoms. The screening is described fairly well by introduction of an effective atomic number, $Z^{-1/3} = (Z_1^{2/3} + Z_2^{2/3})^{-1/2}$, in the formula for the Thomas–Fermi screening radius (Equation 4) (Lindhard, 1965).

In the intermediate range, heavy ions at high velocity but carrying many electrons, the situation is not clear and further studies would be desirable. As discussed below, there is empirical evidence from blocking of fission fragments that in a high-Z material there is only a small contribution from projectile electrons to the screening. On the other hand, observations of "cooling" and "heating" of heavy-ion beams transmitted through thin crystals give clear evidence of an influence of the ion charge state on the interaction potential.

5. Lindhard's Critical Angle

Axial channeling requires incidence nearly parallel to a crystal axis. A limit to the incidence angle ψ is obtained from the expression for the string potential. The transverse momentum of a particle with angle ψ is $p_\perp = p \sin \psi \cong p\psi$ and hence the kinetic energy in the transverse motion is $E\psi^2$. The barrier for penetration into a string is of order $2Z_1 Z_2 e^2/d$ (Equation 5) and hence the critical angle is of order of the Lindhard angle,

$$\psi_1 = \left(\frac{2Z_1 Z_2 e^2}{Ed} \right)^{1/2} . \tag{7}$$

For relativistic particles with total energy $\gamma M_1 c^2$, the kinetic energy in the transverse motion turns out to be $p_\perp^2/2M_1\gamma$ and the formula (7) holds with the replacement $E \to 1/2pv = 1/2\gamma M_1 v^2$ (Lervig et al., 1967).

Lindhard introduced the rough distinction between "aligned beam" ($\psi < \psi_1$) and "random beam" ($\psi > \psi_1$). Transition from aligned to random is denoted "dechanneling" and the reverse transition "feeding-in". For random beam many aspects of the motion are like in an amorphous medium because there is no restriction of the transverse motion. However, at very high energies the correlated scattering with string atoms extends to angles much larger than the critical angle and this has important consequences, for example for the multiple scattering and for radiation from electrons and positrons.

6. Thermal Vibrations

Thermal vibrations play an important role. On the time scale of the ion motion the displacements of atoms can be considered static. The atomic recoil can be ignored in the evaluation of the scattering angle and, except for questions of coherence in electron channeling, we need not be concerned about the quantisation of atomic motion into phonons. The rms vibrational amplitude in two dimensions, ρ, is typically of order 0.1 Å. When a particle can penetrate to a distance of order ρ from strings it is able to hit atoms. With a Gaussian distribution of the thermal displacements r, $\mathrm{d}P(r) = \exp(-r^2/\rho^2)\ \mathrm{d}r^2/\rho^2$, an ion with minimum distance of approach to strings equal to $\rho\sqrt{\ln 2}$ will have the probability for a head-on collision with an atom reduced by a factor of two compared with an amorphous target. A more precise estimate of the critical angle is therefore

$$\psi_c = \left(\frac{U(\rho\sqrt{\ln 2})}{E}\right)^{1/2}. \tag{8}$$

With the standard potential in Equation (5) we obtain

$$\psi_c = \psi_1\left[\frac{1}{2}\ln\left(\frac{(Ca)^2}{\rho^2 \ln 2} + 1\right)\right]^{1/2}. \tag{9}$$

The factor on ψ_1 is close to unity.

The vibrational displacements also modify the continuum potential. Instead of the logarithmic divergence at small r the thermally averaged potential U_T has a finite maximum at $r = 0$, close to $U(\rho/\sqrt{2})$, but replacement of U by U_T leads to only a very small change in Equation (9) (Andersen and Feldman, 1970).

7. Dip in Yield

The most dramatic consequence of channeling is the nearly complete extinction of processes requiring a small impact parameter with a crystal atom. As illustrated in Figure 5, the yield of such a process, normalised to the yield in an amorphous medium, is strongly reduced for angles of incidence smaller than the critical angle. Particles incident at zero angle and at distance r from a string acquire a transverse energy $U(r)$ and can later hit a fraction $\exp(-r^2/\rho^2)$ of the vibrating atoms. With the assumption of a rapid trend towards statistical equilibrium in the allowed area (a uniform distribution), we therefore obtain

$$\chi_{\min} = \frac{1}{A_0}\int_{A_0} 2\pi r\ \mathrm{d}r \exp(-r^2/\rho^2) = \pi\rho^2/A_0. \tag{10}$$

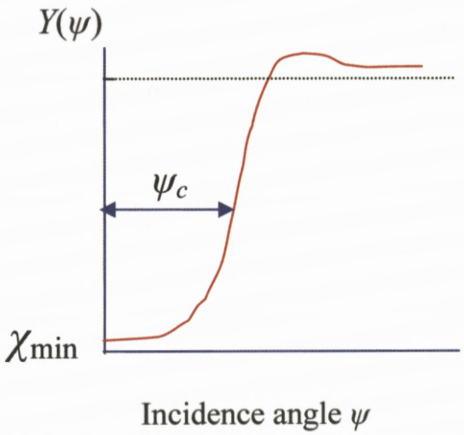

Figure 5. Axial dip in close-encounter yield.

The minimum yield χ_{min} is of order $\leq 1\%$, only. Roughly, the result may be interpreted as immediate dechanneling of the ions which hit the surface inside a distance ρ from a string. As discussed below, there are corrections, mainly due to effects of crystal planes containing the axis, which increase the minimum yield by a factor of order 3, the so-called Barrett factor first established in computer simulations (Barrett, 1973a).

Since recoils can be ignored the particle trajectories can be calculated as motion in a fixed potential. They are reversible in time if energy loss can be ignored, and this has several important consequences. One is the equivalence between channeling and blocking. Blocking occurs when charged particles are emitted from a lattice site in an axial direction, as illustrated in Figure 6. The emitted particles are blocked by the string and prevented from exiting the crystal in the axial direction. Reversibility implies that the width and minimum yield of the blocking dip are identical to those for the channeling dip. Pioneering work on blocking was carried out especially by Tulinov and his group in Moscow (Tulinov et al., 1965).

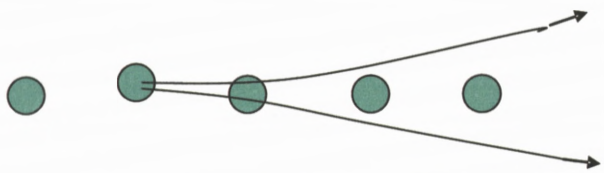

Figure 6. Blocking in the direction of a string of particles emitted from a lattice site.

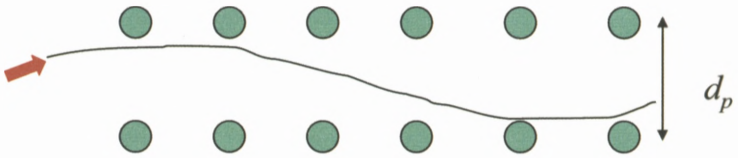

Figure 7. Planar channeling.

8. Planar Channeling

Also for particles incident on a crystal nearly parallel to a major crystallographic plane the motion can be guided by a continuum potential, given by

$$V(x) = Nd_p \int \mathrm{d}y\, \mathrm{d}z\, V_{\mathrm{at}}(x, y, z) \tag{11}$$

for a plane with spacing d_p. The density of atoms in a plane is Nd_p.

The critical angle for planar channeling is smaller by a factor of order 3 than for axial channeling. The motion is one-dimensional oscillation, as illustrated in Figure 7. Planar channeling gives rise to a dip in yield, with a narrower width and a higher minimum yield than for axial channeling. Planar effects are therefore normally less useful for applications. At very high energies, planar channeling in a bent crystal can be used to bend beams of charged particles, as first suggested by Tsyganov.

A special situation is the motion of particles nearly parallel to a set of close-packed strings in the plane. The planar channeling in this region, which Lindhard called channeling by a string of strings, is weakened because the particles can penetrate the planes between the strings. As we shall discuss below, channeling by planes is still important for the behaviour of axially channeled particles and it is a major cause of the Barrett factor on minimum yields mentioned above.

9. Channeling of Electrons and Positrons

An important issue is the question whether classical mechanics can be applied to describe ion channeling. Lindhard carried out an elegant analysis analogous to Bohr's famous argument concerning the use of classical orbital pictures in binary Coulomb scattering, which leads to the condition

$$\kappa = \frac{2Z_1 Z_2 e^2}{\hbar v} > 1, \tag{12}$$

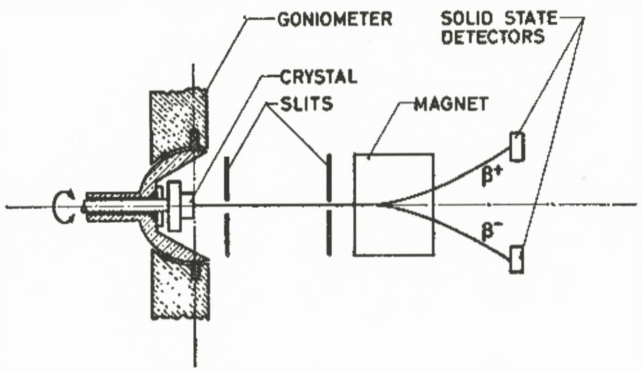

Figure 8. Set-up for observation of the emission of electrons and positrons from ^{64}Cu implanted into a copper crystal (Uggerhøj and Andersen, 1968).

where v is the projectile velocity. For correlated scattering on string atoms it was shown that for particles heavy compared with the electron the transverse motion is always classical. A particle scattering off a string can be described by a wave packet with extension small enough to give a well defined scattering angle and still large enough for the spread in direction of the motion, deriving from the uncertainty principle, to be insignificant. Qualitatively, the reason is that the parameter Z_2 in the above formula, giving the strength of the scattering potential, is in effect increased by the concerted participation of many string atoms.

Channeling of electrons and positrons was hotly debated in the late sixties and early seventies. The essentially classical features of blocking of electrons and positrons were demonstrated by Uggerhøj by observation of the emission of both particles from radioactive ^{64}Cu implanted into a copper crystal (Uggerhøj, 1966; Uggerhøj and Andersen, 1968). The beautifully simple experiment is illustrated in Figures 8 and 9. The crystal is mounted in a goniometer and two collimators determine the emission direction for both electrons and positrons. As shown in Figure 9, there is a strong decrease in yield along the axis for positrons, similar to observations for heavier particles like alpha particles. In contrast, there is a strong increase in the yield of electrons, as would be expected classically from the reversed sign of the interaction with string atoms.

The classical interpretation of these experiments was criticised and it was argued that, as known from electron microscopy, the transmission of electrons through thin crystals is dominated by coherent Bragg reflection. However, it was soon realised that this quantisation of transverse momentum does not in itself imply the absence of strong classical features. The decisive question is again whether the localisation of an electron to move close to a string or plane gives too much

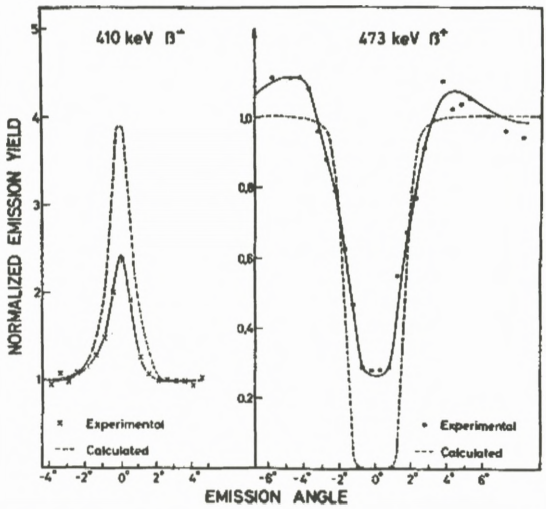

Figure 9. Observed yields along an axis, compared with continuum model calculations (Uggerhøj and Andersen, 1968).

spread in direction of motion via the uncertainty principle to allow a classical description by orbital pictures. This is determined by the number of bound states in the transverse motion, which becomes large for relativistic electrons (Gemmell, 1974; Andersen et al., 1977).

The phase space for bound states in a planar potential is larger for positrons, which oscillate in the open space between planes, and hence channeling is more classical for positrons than for electrons. Figure 10 shows a comparison between a measured planar dip in yield of wide-angle scattering for 1.2 MeV positrons and a so-called many-beam quantum calculation (Pedersen et al., 1972). The dip has an essentially classical envelope with fine structure from Bragg interference.

10. Channeling Radiation

The discovery of channeling radiation should be accredited mainly to Kumakhov, who was the first to derive the correct relativistic transformation (Kumakhov, 1976). The simplest way is to consider first the emission of radiation in the so-called rest system following the electron motion along a string or plane, and then make a Doppler transformation to the laboratory system. The outcome is that the Bohr relation between the photon frequency and the electron energy jump is modified by approximately a factor $2\gamma^2$ for emission in the forward direction. A line spectrum of planar channeling radiation was first presented by the Livermore

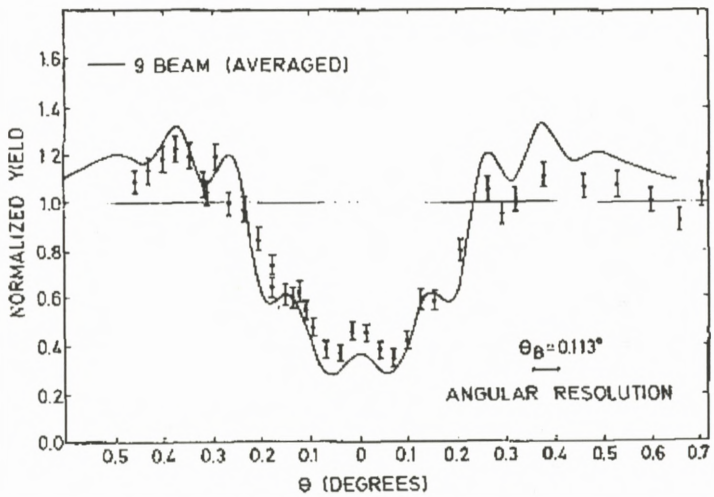

Figure 10. Wide-angle scattering near a (110) plane for 1.2 MeV positrons in Si, compared with a many-beam calculation (Pedersen et al., 1972).

group at the ICACS conference in Hamilton, 1979 (Alguard et al., 1980), and shortly afterwards we observed in Aarhus the first line spectra for axially channeled electrons (Andersen and Lægsgaard, 1980). As illustrated by the spectrum in Figure 11, the lines of channeling radiation are particularly sharp in diamond because of low Z and small thermal vibrations in this material (Guanere et al., 1982).

For not too high energies (MeV) a quantum treatment must be applied, and a systematic description can be based on the formalism developed by Lindhard and co-workers (Lervig et al., 1967; Andersen et al., 1983a). Spin effects are not important and the Klein–Gordon equation for a spinless particle with charge e and rest mass m may be used as a starting point,

$$\left\{\left[-i\hbar\nabla - \frac{e}{c}\vec{A}(\vec{R})\right]^2 c^2 + m^2c^4\right\}\psi(\vec{R},\ldots)$$
$$= [E - H_{\text{rad}} - H_{\text{latt}} - V(\vec{R},\ldots)]^2\psi(\vec{R},\ldots)\,. \tag{13}$$

Here E is the total energy of the system, and the terms H_{rad} and H_{latt} are the independent Hamiltonians of the radiation field and the crystal lattice, while $\vec{A}$ represents the vector potential of the radiation field. The trick is now to separate off a phase factor,

$$\psi(\vec{R},\ldots) = e^{iKz}\,w(\vec{r},z,\ldots), \quad \text{with} \quad \hbar^2K^2c^2 + m^2c^4 = E^2. \tag{14}$$

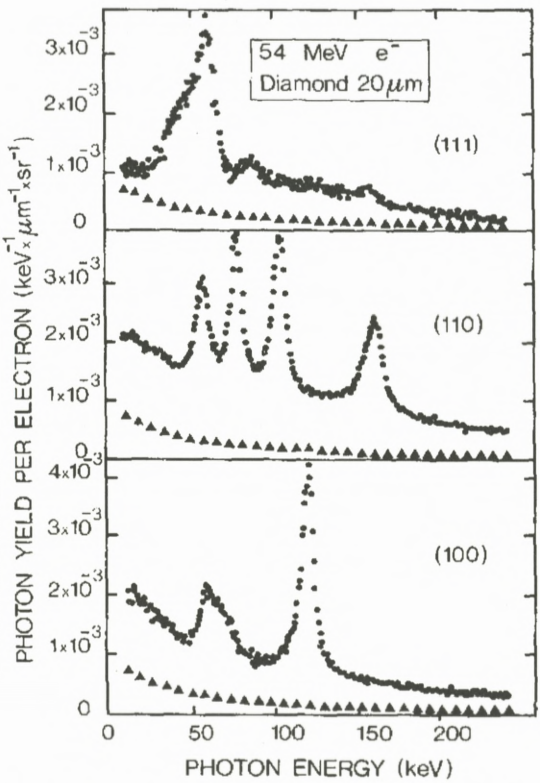

Figure 11. Photon spectra in the beam direction for 54 MeV electrons along different planes in diamond. Triangles show spectrum for incidence in a random direction (Guanere et al., 1982).

This gives an approximate equation of first order in a time parameter $t = z/v$, where v is the velocity corresponding to momentum $\hbar K$. Neglecting terms of second order, like $\partial^2/\partial z^2$ and V^2, we obtain

$$i\hbar \frac{\partial}{\partial t} w = \left[-\frac{\hbar^2}{2\gamma m} \Delta_r + V(\vec{r}, t, \ldots) + H_{\text{rad}} + H_{\text{latt}} + H_{e,r} \right] w(\vec{r}, t, \ldots)$$

$$H_{e,r} = -e \left(\beta A_z + \frac{1}{\gamma mc} \vec{A} \cdot \vec{p} \right). \tag{15}$$

The equation has the form of a non-relativistic Schrödinger equation in two dimensions, and the wave function describes the transverse channeling state. The radiation operator $H_{e,r}$ can be treated as a perturbation, and also the interaction potential can be simplified by a series of perturbation approximations. For example, the electronic excitations are treated by a replacement of V by its expectation

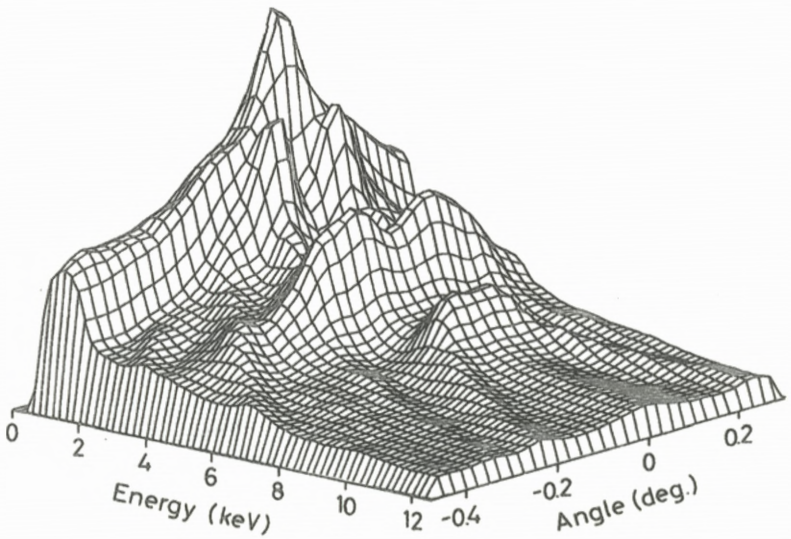

Figure 12. Photon spectra *versus* angle of incidence to a ⟨111⟩ axis for 4 MeV electrons in a 0.5 μm thick Si crystal (Andersen et al., 1982).

value $\langle V \rangle$ in the electronic ground state and a perturbation calculation of the inelastic transitions induced by the difference $V - \langle V \rangle$. Similarly, vibrational excitations of the lattice are treated by the introduction of a thermally averaged potential, with Fourier components reduced by a Debye–Waller factor. In the final step, the potential is approximated by the thermally averaged axial or planar continuum potential.

Measurements of axial channeling radiation for 4 MeV electrons along a Si⟨111⟩ direction are shown in Figure 12 (Andersen et al., 1982). In analogy to atomic states, the bound states may be labelled as s, p, d, ... with angular momentum 0, 1, 2, ... Four lines are clearly distinguished, from 2s–2p, 3d–2p, 2p–1s, and 3p–1s transitions. The angular dependence of the intensities reflects the overlap of the incoming plane wave with the initial states of the transitions, i.e., the intensity is proportional to the square of a Fourier component of the transverse wave function. The ridges at larger angles are from free-to-bound transitions.

Radiative transitions between the bound levels give photon energies in the direction of the axis equal to $h\nu = 2\gamma \Delta E_R$, where E_R is the energy level in the reference system moving with the particle in the z direction, the so-called rest system. Here the mass is non-relativistic and the potential is multiplied by a factor of γ due to the Lorentz contraction of the spacing, d, of atoms on a string. Hence the Hamiltonian is just multiplied by the factor γ. The measurements are in

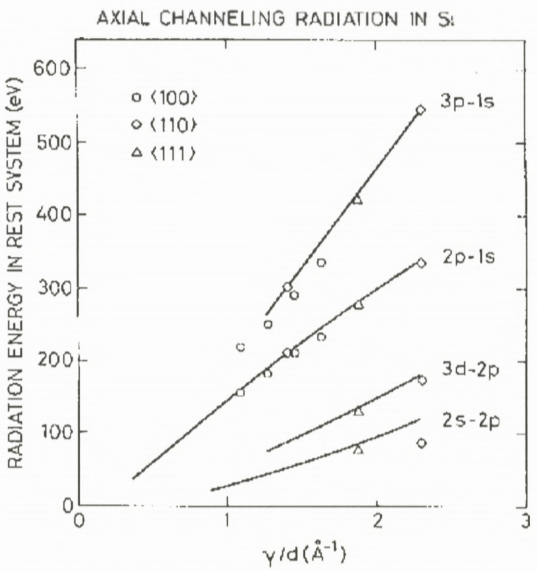

Figure 13. Comparison between calculated transition energies in the rest frame and measurements, at varying electron energy, $E = \gamma mc^2$, and for axes with different atomic spacing, d (Andersen et al., 1982).

Figure 13 seen to be reproduced quite well by calculations. Transitions along three different axes are included. The potential scales with γ/d (Equation 3) and hence measurements for channeling along three different axes can be included in one graph with scaled units. The agreement is quite good when an accurate potential (Doyle–Turner, for example) is used.

The line spectrum of channeling radiation reveals the energy spectrum of bound states, just like the Rydberg series revealed to Niels Bohr the discrete states of the hydrogen atom. Observation of the energies combined with the perturbation calculations can give quite accurate information about crystal properties like the crystal potential and the thermal vibrations (Datz et al., 1986; Hau et al., 1990). It is also possible to calculate the coherence properties from up to third order perturbation theory and reproduce the observed line widths (Andersen et al., 1983b; Hau and Andersen, 1993a, 1993b).

After a hectic period in the 1980s with many active groups, both in theory and in experiments, the activity in low-energy channeling radiation has subsided, and today it is rare to see a paper in this field. Perhaps the field is too well established. Also, the early promises of application of MeV electron beams in crystals as a radiation source seem not to have materialised. In contrast, there has been a

continued interest in radiation phenomena in crystals for high-energy electrons (GeV). The physics in this region is very different, with essentially classical motion of the electrons, and other processes like creation of particle-antiparticle pairs have been studied. The photon yield can be very strongly enhanced and, like the Bethe–Heitler bremsstrahlung spectrum for an amorphous medium, the radiation spectrum extends up to the kinetic energy of the particle. The production of hard photons for particle physics is therefore an interesting application. The effective electrical field generating the radiation corresponds to the continuum potential in the "rest system", and since it is proportional to the relativistic factor γ it becomes huge at extreme relativistic energies. This opens up for fundamental studies in strong-field electrodynamics (Uggerhøj, 2005).

11. Dechanneling

Multiple scattering is strongly reduced for channeled particles. There remain force fluctuations due to thermal vibrations and electronic scattering. One can derive a differential equation for the distribution in transverse energy, $g(E_\perp, z)$, as a function of the depth z (Beloshitsky et al., 1972; Bonderup et al., 1972),

$$\frac{\partial}{\partial z} g(E_\perp, z) = \frac{\partial}{\partial E_\perp} A(E_\perp) D(E_\perp) \frac{\partial}{\partial E_\perp} \frac{g(E_\perp, z)}{A(E_\perp)} . \tag{16}$$

This is a diffusion equation with diffusion function $D(E_\perp)$. The equation reproduces the stability of a uniform distribution in phase space, corresponding to a distribution in transverse energy which is proportional to the allowed area, $g_0(E_\perp) \propto A(E_\perp)$. Since the available area is constant at large $E_\perp$, also g_0 becomes constant. This is special for two dimensions. For planar channeling an analogous equation can be derived, with $A(E_\perp)$ replaced by the half-period of oscillation, $T(E_\perp)$. At large angles, $T(E_\perp)$ is the time interval between the crossings of planes and the equilibrium distribution is proportional to $E_\perp^{-1/2}$.

In a perfect crystal, the diffusion is due to scattering by individual electrons and to fluctuations in atomic scattering associated with thermal displacements. In an amorphous target, nuclear multiple scattering dominates. The mean square multiple scattering angle increases linearly with depth (apart from a logarithmic factor) and, as a scaling length, Lindhard introduced the depth corresponding to an rms scattering angle equal to ψ_1,

$$l_{n,\psi_1} = \frac{2}{\pi N d^2 L_n \psi_1^2} , \tag{17}$$

where the logarithmic factor, L_n, is of order 5–10. This length is roughly proportional to the energy of the particle and hence channeling can be stable over very

large thicknesses at high energies. At GeV energies, the dechanneling lengths are macroscopic (centimetres) and planar channeling in bent crystals can be used for beam bending without too much loss (Baurichter et al., 2000).

Lindhard introduced a diffusion equation already in the 1965 paper, but with the transverse momentum vector as variable. Since it is the transverse energy and not the transverse momentum which is conserved in the continuum model (without diffusion), the magnitude of the variable was in reality the square root of the transverse energy (apart from a constant), and the direction of the vector had no physical significance. The two descriptions are then equivalent but, to avoid confusion, it is better to use the transverse energy as variable.

The diffusion equation may be derived from a more general master equation by a second-order expansion in the small jumps in transverse energy. However, this expansion is not unique! By straight-forward expansion, one obtains a differential equation with an additional drift term (Oshiyama and Mannami, 1981). When Bonderup and I first carried out this expansion, we found exactly the same result and thought that we had discovered a rare error in our master's work. Wisely, we decided to celebrate with a beer in the canteen before confronting Jens Lindhard with our result. Sure enough, he had much deeper insight (Lindhard and Nielsen, 1971) and suggested the method of expansion described in our paper (Bonderup et al., 1972). The point was to conserve the detailed balance of scattering in the master equation and thereby keep the correct statistical equilibrium.

An example illustrating the accuracy of the description by diffusion is shown in Figure 14 (Kennedy et al., 1992). In the calculations, an accurate potential was applied and dechanneling by electronic and thermal scattering was included in the diffusion approximation. The two scattering mechanisms complement each other. The thermal fluctuations dominate at large transverse energies and, for example, cause the planar shoulder to be smeared out rapidly. On the other hand, thermal scattering is very weak for well channeled ions, and electronic scattering is therefore important for the increase of the minimum yield with depth of penetration.

12. Dechanneling by Crystal Defects

When dechanneling by defects is included, the diffusion equation may not be suitable. Alternative approaches are solution of a master equation, which can include large jumps in transverse energy (Gärtner et al., 1984), or brute force computer simulation.

The detection of crystal defects after ion implantation has probably been the most important application of channeling. For example, it has been of decisive

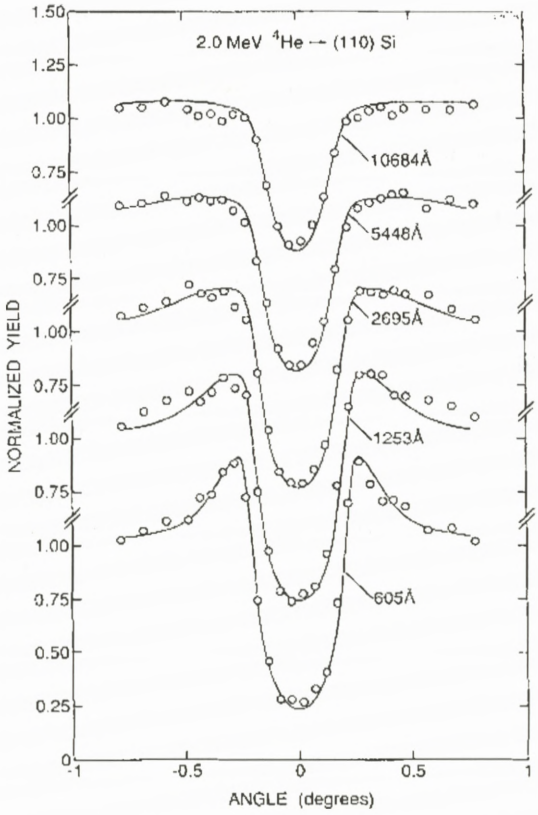

Figure 14. Depth dependence of backscattering for 2 MeV He near a (110) plane in Si, compared with dechanneling calculation (Kennedy et al., 1992).

importance in the development of ion implantation for doping of semiconductors (Mayer et al., 1970). With backscattering of MeV beams of protons or helium ions, the crystal perfection as a function of depth can be measured, as illustrated in Figure 15 (Feldman et al., 1982). The energy scale for the backscattered particles can be converted into a depth scale, as shown at the bottom. The spectrum for a beam aligned with an axis is shown for a virgin crystal as well as for an implanted crystal, and the difference in the yield can be ascribed to a combination of direct backscattering from defects and increased backscattering from atoms in perfect parts of the crystal due to dechanneling. This latter part is indicated by the dashed line and when it is subtracted the depth distribution of the damage is obtained. Methods for analysis of such spectra are today readily available and, all

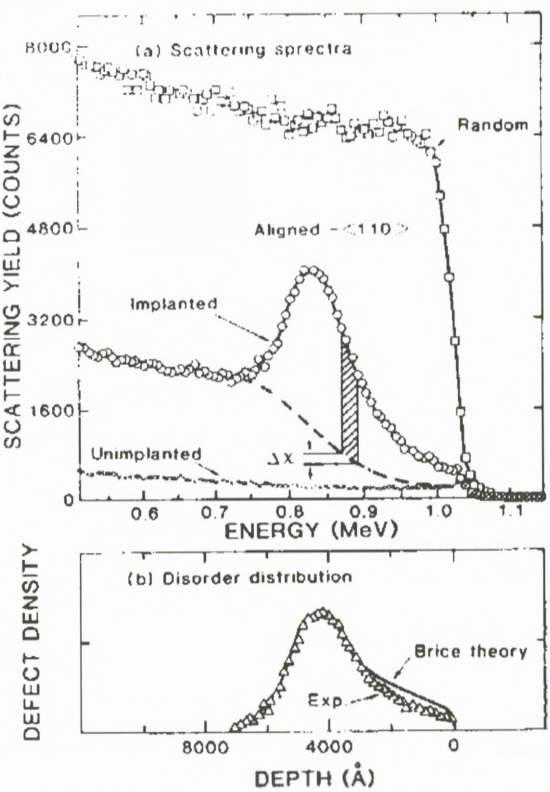

Figure 15. Illustration of the extraction of a damage profile from backscattering in aligned and random directions (Feldman et al., 1982).

in all, dechanneling is a very well developed field, except for the integration of the influence of electron capture and loss by heavy ions to be discussed later.

13. Localisation of Impurities by Channeling and Blocking

Another important application of channeling has been the use of the strong dip in yield of a close-encounter reaction to determine the location of impurity atoms in a crystal lattice. An example is the determination of the lattice configuration of nitrogen implanted into silicon (Berg Rasmussen and Bech Nielsen, 1994). Nitrogen impurities can be detected at low concentrations by a (p, α) reaction. The observed yield of this reaction together with the backscattering yield from the Si lattice is shown in Figure 16 for angular scans through the three major axes.

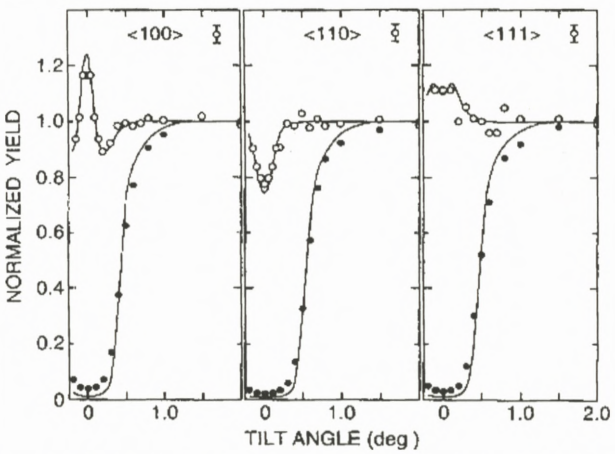

Figure 16. Angular distributions in yield of (p, α) reaction and of backscattering from Si crystal implanted with nitrogen. The lines are from calculations including dechanneling (Berg Rasmussen and Bech Nielsen, 1994).

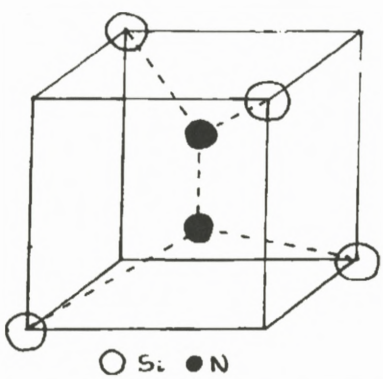

Figure 17. Nitrogen dumb-bell replacing substitutional atom in Si lattice (Berg Ramussen and Bech Nielsen, 1994).

The scans are averaged over the azimuthal angle whereby perturbations by planar effects are largely eliminated.

The data are consistent with the dumb-bell configuration illustrated in Figure 17. Two nitrogen atoms replace one silicon atom. The lines through the data points are from calculations for such a configuration. The dumb-bells are oriented randomly along the three equivalent ⟨100⟩ axes (edges of cube). Nitrogen is substitutional along one axis and interstitial along the other two. This gives a superposition of 1/3 dip and 2/3 narrow peak. An accurate potential (Doyle–

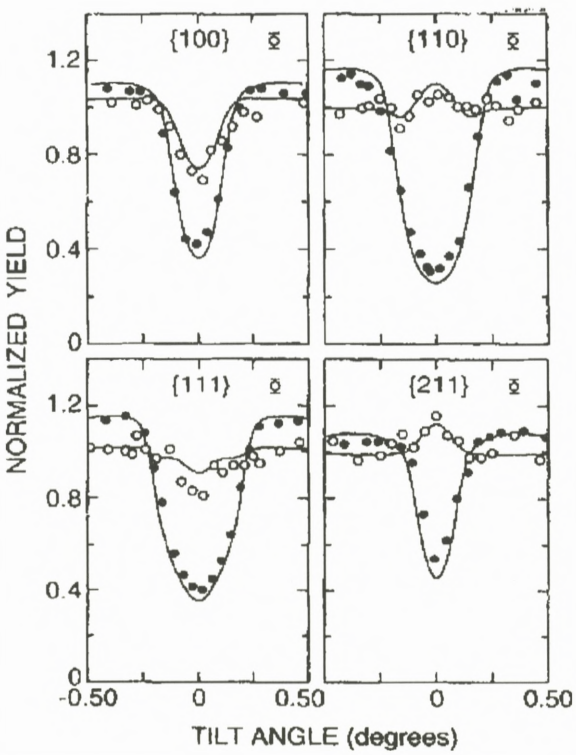

Figure 18. Planar angular scans of (p, α) and backscattering yields for nitrogen implanted Si crystal, compared with calculations including dechanneling (Berg Rasmussen and Bech Nielsen, 1994).

Turner) has been used and dechanneling for a perfect lattice has been included. This is seen to give excellent agreement with the data, both for the impurity and for the host lattice. As seen in Figure 18, also the observed structures for channeling along three different planes were found to be in good agreement with the simulation (planar scans sometimes give crucial information!; Bech Nielsen et al., 1988).

The equivalence of channeling and blocking implies that impurities can just as well be localised by observation of blocking dips for charged particles emitted from the impurity atoms. A very early example is Domeij's observation of a strong blocking dip for α-particles from ^{222}Rn implanted into a tungsten crystal (Domeij and Björkqvist, 1965). The measurements on electrons and positrons discussed above showed that information on lattice location can also be obtained from observation of the blocking effects for these light particles. This is very useful since

beta emitting isotopes are ubiquitous in the periodic table. A pioneering effort on quantitative application of this method has been made by Hofsäss (1996).

14. Crystal Blocking for Determination of Nuclear Lifetimes

In analogy to the lattice localisation of impurities the blocking effect can be used to determine how far from a lattice site the emission of charged particles takes place. For a nuclear reaction proceeding by formation of a compound nucleus, one may thereby determine the average recoil distance $v_\perp \tau$, where $v_\perp$ is the component of the compound nucleus velocity perpendicular to the axis and τ is the compound nucleus lifetime (Gibson, 1975).

Several groups have studied fission lifetimes with this technique. Since the early seventies I have been working with a group mainly from Aarhus and from the Chalk River Nuclear Laboratories on the development of this technique to study heavy ion induced fission of heavy nuclei. Because the recoil is large in these reactions, very short times can be measured, down to about one attosecond. This is still very long on the nuclear time scale and times of order 10^{-21} s are expected from statistical models at the very high excitation energies just after formation of a compound nucleus. In a series of experiments with C, O, and F projectiles on W and Ta crystals, we found results consistent with this expectation. No narrowing of the dips was found but there was an increase in the minimum yield compared with dips in elastic scattering. As illustrated in Figure 19, the results could be fitted with a superposition of mostly fast fission without lifetime effects and a contribution from slow fission after cooling down of the nucleus by emission of several neutrons (Andersen et al., 1976). The measurements for different crystal temperatures and thicknesses are examples of the experimental tests carried out to ensure that the increase in minimum yield was not due to an artefact as, for example, stronger dechanneling for fission fragments than for scattered ions. Additional confirmation was obtained from a variation of the bombarding energy: at higher energies the dips become nearly identical to the blocking dips for scattered ions, scaled in angle with $(Z_1/E)^{1/2}$ according to Equation (7).

Recently we have continued the experiments with heavier projectiles. The idea is to investigate the influence of viscosity on the nuclear mass flow at high internal temperatures. Results from other types of measurements, e.g., on the number of neutrons emitted prior to fission and on emission of giant-dipole gamma rays from the compound nucleus, have indicated that the lifetime can be rather long. The first measurements with 170–180 MeV ^{32}S projectiles gave fission blocking dips which were virtually identical to scaled dips in elastic backscattering (Karamian

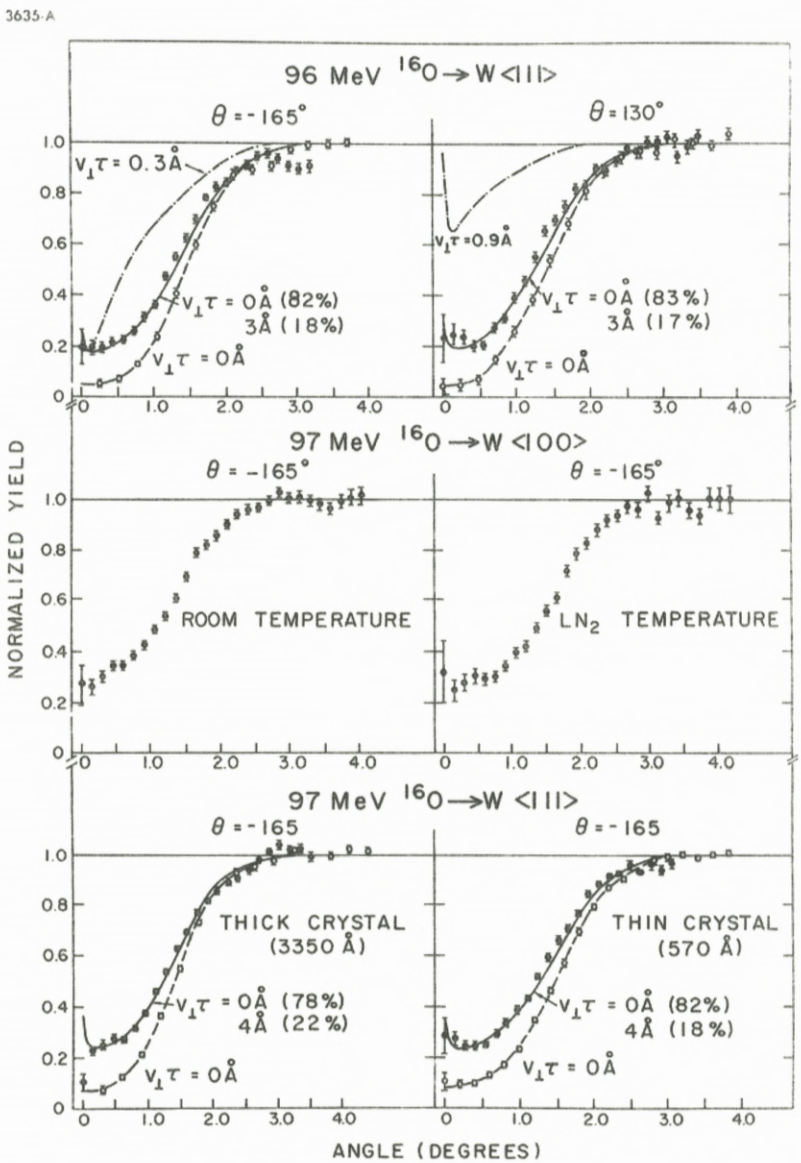

Figure 19. Blocking dips for fission fragments (filled squares) and scaled dips in elastic scattering for ^{16}O bombardment of thin tungsten crystals. The fission dips have been fitted with two components, one for very short recoil represented by the elastic dip and the other a calculated dip for a very large average recoil distance. The top left figure includes a calculation for a single lifetime with intermediate recoil distance (0.3 Å). It reproduces the minimum yield but not the width (Andersen et al., 1980).

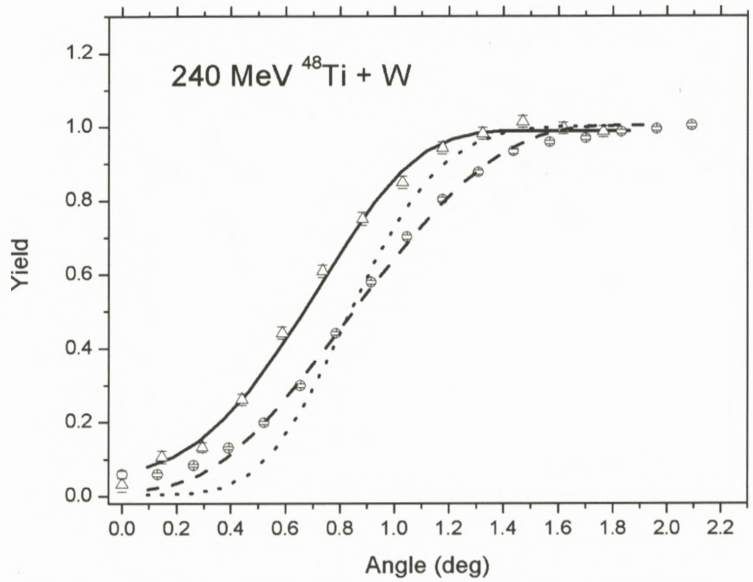

Figure 20. Blocking dip for fission fragments (triangles) and a scaled dip in elastic scattering (circles), compared with continuum-model calculations, including a correction for angular resolution, which is largest for the elastic dip. The dotted curve is for fission fragments with zero recoil while the full-drawn curve includes an exponential distribution of recoils with average displacement 0.14 Å (Forster et al., 2006).

et al., 2003). This indicates that the lifetime of the fission is below about 1 as and there is no component larger than about 1% with much longer lifetime.

A comparison with elastic backscattering is a very useful zero-lifetime normalisation. However, it is actually somewhat surprising that the agreement is so close since the fission fragments carry many electrons which should contribute to the screening of the Coulomb interaction with tungsten nuclei. Also in earlier experiments with oxygen projectiles the scaling was found to be quite accurate, as seen in Figure 19.

Very recently we have continued these experiments at Oak Ridge National Labs with even heavier projectiles, ^{44}Ti at about 240 MeV (Forster et al., 2006). The analysis indicates a clear narrowing of the fission dip compared with the scaled dip in elastic scattering. This is quite exciting because the time delay must be very long, of order 10^{-18} s, and a large fraction of the fission events must experience this delay. In Figure 20 the results for one bombarding energy are compared with a calculation for an exponential decay with an average displacement of 0.14 Å. The scaled elastic dip is seen to be in excellent agreement with the calcula-

tion for zero displacement, except for a small difference in the minimum yield that can be ascribed to crystal defects. Because the critical angle is smaller by nearly a factor of two for the scattered projectiles compared with fission fragments, the angular resolution is poorer. Hence the fission dip should be compared with the dotted curve calculated with the same resolution as for the fission fragments. The lifetime effect is very clear and the displacement corresponds to a lifetime of about 3 as. This signals a very high viscosity of the nuclear mass flow in the fission process. The physical picture of the united nucleus must correspond to a drop of syrup rather than of water. These results may also be important for the interpretation of recent, very surprising observations of long fission lifetimes for superheavy compound nuclei created in heavy-ion reactions (Drouart et al., 2005).

The observations shown in Figures 19 and 20 are also interesting from a methodological point of view. They give a clear demonstration of the power of the technique to determine not only average displacements but also the distribution of displacements. The observation in Figure 20 shows that small displacements from a lattice site are most easily detected by the narrowing of the width of the blocking (or channeling) dip, rather than by the increase of the minimum yield. The surprising accuracy of the scaling of the elastic dips is a problem which deserves theoretical and perhaps also further experimental study.

15. Restricted Equilibrium in Axial Channeling

All through the history of channeling, computer simulation has played a prominent role. The earliest ideas were inspired by simulation of the penetration of low-energy ions through crystals, and simulation is still a very valuable tool for interpretation of experiments. Probably the most advanced code was developed by John Barrett at Oak Ridge and he made important contributions to the theory of channeling on the basis of simulations. An example is the observation that the minimum yield in the axial channeling dip is underestimated by a factor of two to three, the so-called Barrett factor (Barrett, 1973a). His search for an explanation of this factor led him to publish a paper with the title: "Breakdown of the Statistical-Equilibrium Hypothesis in Channeling" (Barrett, 1973b).

The basic observation is illustrated in Figure 21. The lines indicate simulated (transverse) trajectories of ions incident on a crystal parallel to an axis and hitting the surface close to a string. In the transverse motion, the ions are accelerated away from this string and their transverse energy, $\varepsilon \equiv E_\perp$, is given for each picture. The strings are indicated by dots, and the figure shows that the flux of ions tends to be focussed onto other strings. This focussing clearly violates the assumption of

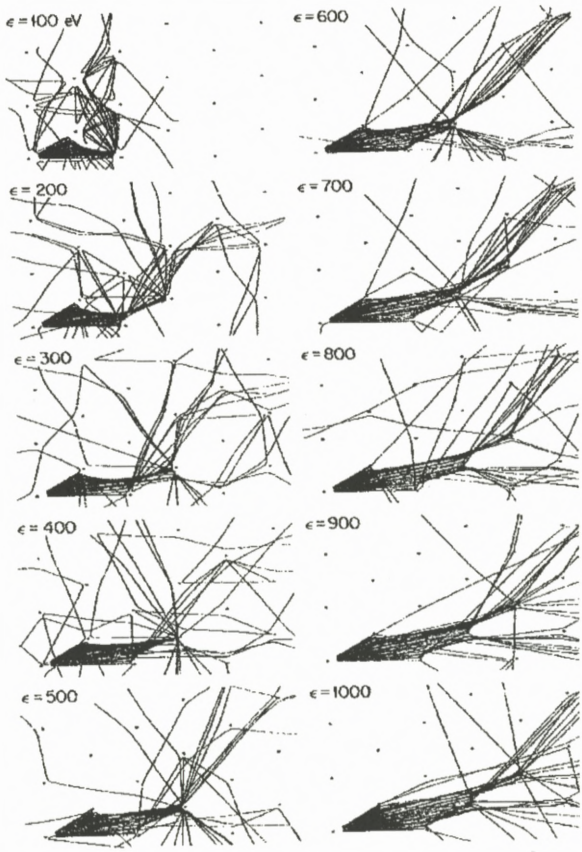

Figure 21. Projection onto (111) plane of trajectories of 3-MeV protons moving nearly parallel to [111] direction in tungsten at 1200 K (Barrett, 1973b).

a rapid trend towards statistical equilibrium on an energy shell in the transverse phase space.

This paper appeared to be a heavy blow to Lindhard's theory of channeling, in which, as noted above, arguments based on statistical equilibrium play a key role. The problem must be rooted in a restriction in phase space hindering the establishment of a full equilibrium. Typically, such a hindrance is associated with a symmetry and a corresponding conservation law, like for instance conservation of angular momentum for a system with rotational symmetry. For axial channeling, the symmetry is the regular arrangement of the strings in a two-dimensional lattice, and the conservation law is the conservation of transverse energy with respect to planes for ions moving nearly parallel to the planes.

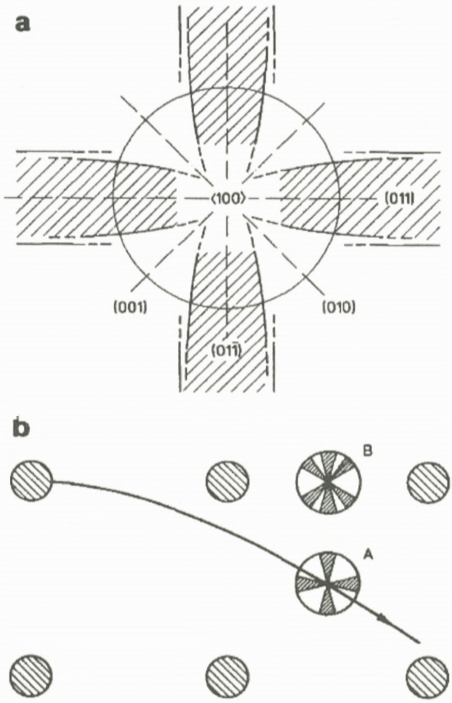

Figure 22. (a) Stereogram indicating regions of planar channeling near a ⟨100⟩ axis in Si, for a particle at position A below. (b) Transverse plane for Si ⟨100⟩. The blocked angular regions are indicated for two positions A and B, and a trajectory for a particle moving out radially from a string is shown (Andersen and Uguzzoni, 1990).

This is illustrated in Figure 22a, showing a stereogram of a small angular region around a ⟨100⟩ direction in a cubic lattice. The major planes containing the axis are indicated, and the circle shows the boundary for axial channeling at the angle ψ_1. Well outside the circle, planar channeling takes place inside the full drawn lines parallel to the plane, but close to the axis planar channeling is replaced by the so-called string-of-strings channeling with a critical angle decreasing with decreasing angle to the axis (Lindhard, 1965). The regions of channeling with respect to the strongest planes are hatched. Very close to the axis, the concept of planar channeling loses its meaning entirely.

Planar channeling divides the transverse phase space into regions with poor communication. An ion in the hatched region remains there on a depth scale determined by planar dechanneling and, *vice versa*, an ion outside the hatched area is prevented from entering this area by scattering on strings. Figure 22b illustrates how we can understand Barrett's results from this division. An ion starting

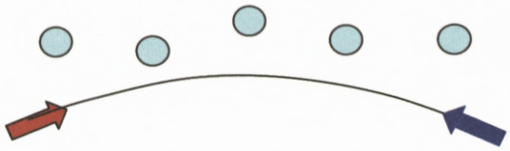

Figure 23. Reversibility of string collision.

its trajectory very close to a string is blocked from the regions of phase space corresponding to planar channeling. As indicated by the two small stereograms embedded in the figure, the blocked angular region depends on the position in the transverse plane. In the accessible, restricted phase space, we may assume a rapid trend towards equilibrium. Compared with a full equilibrium, the probability for getting very close to a string again is then higher by the ratio of the four dimensional volume of the full phase space to the volume of the restricted phase space.

These ideas were supported by simulations (Andersen and Uguzzoni, 1990) and appear to account quite well for a major part of the Barrett factor (Uguzzoni et al., 2000). There is an additional contribution from strong thermal fluctuations in the first collision with a string at the crystal surface, which determines the transverse energy of the ions giving the minimum yield. Thus the first attack on the concept of statistical equilibrium in channeling was repelled and in the process new insight was gained.

16. Cooling and Heating in Ion Transmission Through Crystals

The second attack on statistical equilibrium in channeling was of an even more fundamental nature. As noted above, it is an important constraint in the derivation of the diffusion equation for dechanneling that a constant density in phase space should be an equilibrium. The phase space is now not limited to a transverse-energy shell but extends out to angles much larger than the critical angle. The requirement follows from basic symmetries of the multiple scattering.

Consider for example the thermal scattering of an ion colliding with a string, as illustrated in Figure 23. If the energy loss in the collision is ignored, the trajectory is reversible, and this implies that thermal scattering leading from $E_\perp$ to $E'_\perp$ has the same probability as scattering from $E'_\perp$ to $E_\perp$. It is easy to see that the same symmetry must hold for changes in transverse energy due to electronic collisions. Until recently, it was believed that the only deviations from this general rule were due to energy loss of the projectile and that they must be small. The observations to be described in the following therefore came as a great surprise.

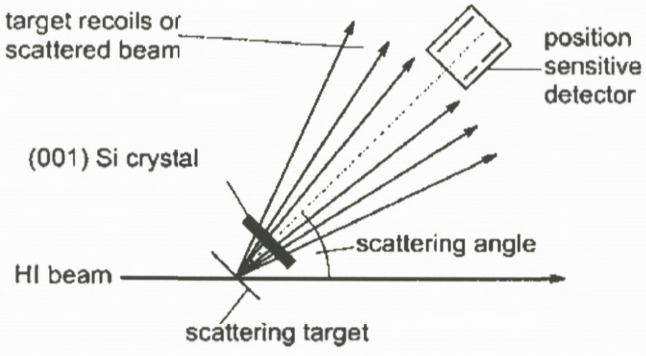

Figure 24. Geometry for transmission experiment (Assmann et al., 1999).

The set up shown in Figure 24 was designed by Assmann et al. to give a sensitive test of the equilibrium hypothesis for heavy ions transmitted through a thin crystal (Assmann et al., 1999). By scattering of a heavy-ion beam in a thin foil, a thin Si crystal was illuminated with a beam with large angular divergence, and behind the crystal the angular distribution of the ions was measured with a position sensitive detector. An isotropic beam with uniform intensity gives a constant distribution in transverse phase space inside the crystal, and if this distribution is stable, the beam will remain isotropic after the passage of the crystal.

The results shown in Figure 25 are dramatically different. To the left are the two-dimensional intensity distributions and to the right the azimuthally averaged intensity as a function of the angle to the axis. For carbon ions there is a strong accumulation of flux near the axis and the planes, denoted cooling. The transmission of Cu ions is an intermediate case, with cooling along the axis and the strongest planes but a depletion of the flux ("heating") along the weaker planes. For transmission of the heavier iodine ions, there is almost exclusively heating, and for the heaviest Au ions there is strong heating along all channeling directions.

Assmann first told me about his strange results at a conference on ion beam analysis (IBA 1995) in Phoenix, Arizona. It was clear that the underlying mechanism must violate the detailed balance of multiple scattering which secures stability of a uniform distribution in phase space. I later discussed this problem with Jens Lindhard, and we agreed that irreversible energy-loss processes must be responsible. However, after our discussion in Phoenix, Assmann modified his setup to the one illustrated in Figure 24 and obtained the striking results shown in Figure 25. It was easy to estimate the magnitude of effects due to energy loss processes, and the observed effects were clearly much larger.

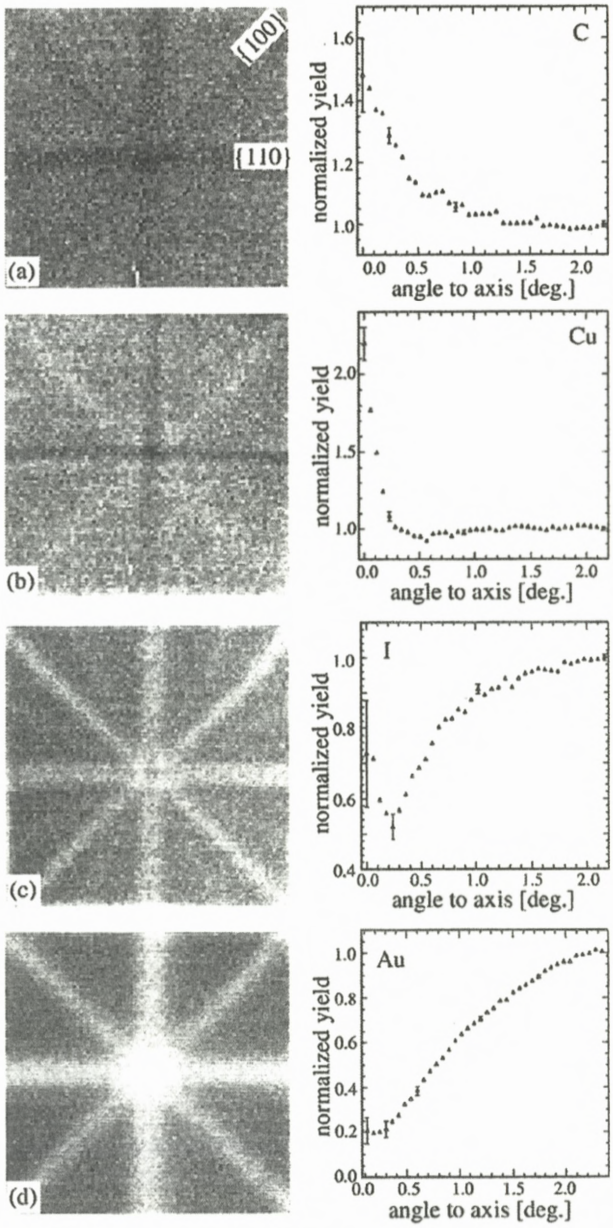

Figure 25. Flux distributions of heavy ions after transmission through (001) Si crystal. To the right azimuthally averaged intensities; (a) C recoils at 18 MeV after 8.7 μm; (b) Cu recoils at 46 MeV after 8.7 μm; (c) scattered I ions at 121 MeV after 2.9 μm; and (d) scattered Au ions at 92 MeV after 2.9 μm. The angular range is $\pm 2.2°$ (Assmann et al., 1999).

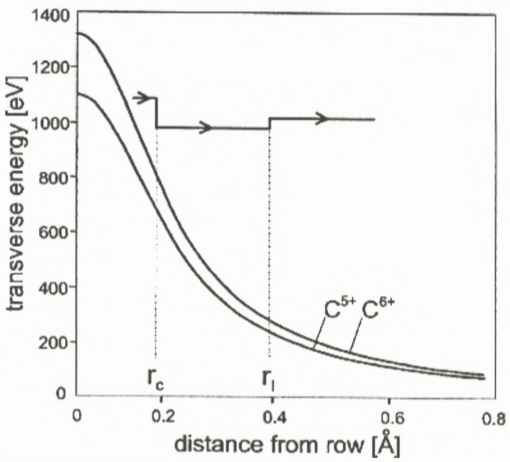

Figure 26. ⟨100⟩ Si string potentials for C^{5+} and C^{6+} ions, in the point-charge approximation (Equation 6). The horizontal line indicates the transverse energy of an ion capturing an electron at r_c and losing it at r_l (Assmann et al., 1999).

In the search for an explanation the requirement of microscopic irreversibility was the decisive clue. In addition to energy loss, also changes of the ion charge due to capture or loss of electrons are irreversible processes. Electrons bound to crystal atoms are captured and ion electrons are lost into empty states of free motion through the crystal. Furthermore, electron capture or loss can change the transverse energy of an ion. For highly stripped ions the effective continuum potential is proportional to the net charge of the ion (Equation 6). Electron capture then leads to a reduction of the transverse potential energy and electron loss to an increase. If, on the average, electron capture takes place at smaller distances from strings than electron loss there will be a net cooling effect, and this is indeed predicted to be the case at very high velocities, from the known impact-parameter dependencies of capture and loss in this limit.

The mechanism is illustrated in Figure 26. A C^{6+} ion is moving away from a string with transverse energy close to 1100 eV. At the distance r_c it captures an electron and loses the transverse energy $U^{(1)}(r_c)$. Later at a distance r_l the electron is lost again and the transverse energy $U^{(1)}(r_l)$ is gained. The cycle has led to a net loss of transverse energy, i.e., to cooling. This mechanism was shown to account qualitatively for the phenomena illustrated in Figure 25. However, it remains a challenge to explain in detail the quite complicated results of later experiments, in particular the observed transition with decreasing velocity from a flux enhance-

ment along channeling directions (cooling) to a flux depletion (heating) (Grüner et al., 2003).

These phenomena clearly offer an opportunity to study the impact parameter dependence of capture and loss processes. The information obtained with the experimental conditions illustrated in Figure 24 is complementary to that gathered from experiments with well defined incidence angle of the ion beam, which yield more detailed data on cross sections (Datz et al., 1972). In order to derive information on charge exchange processes it is necessary to establish a theoretical framework for data analysis. For example, the dependence of the channeling potential on ion charge must be investigated. Only for ions carrying few tightly bound electrons can this dependence be described in the simple manner indicated in Equation (6).

Another problem is to incorporate the capture and loss processes into the dechanneling formalism. The angular distribution of transmitted ions results from a competition between cooling/heating from capture and loss and multiple scattering, which drives the distribution towards isotropy. A first attempt has been made recently (Malyshevsky, 2005). However, it does not include properly the mechanism discussed above. I believe that this is partly because the transverse momentum is used as variable in the description. As discussed in Section 11, this can lead to confusion.

17. Energy Loss for Channeled Particles

We shall now turn to aspects of channeling which Lindhard denoted secondary phenomena, i.e., phenomena which are influenced by channeling but do not in turn affect the steering of the ions very much. The most prominent example is stopping. Studies of ion ranges, both computer simulations and range measurements, played a very important part in the discovery of channeling (see, for example, the introduction to Eriksson et al., 1967). The energy loss to atomic recoils, the so-called nuclear energy loss, is reduced most by channeling, and very long ranges of low-energy heavy ions were observed for incidence parallel to an axis in a crystal.

The selection by channeling of large impact parameters with atoms makes it possible to study the electronic energy loss at low velocities where nuclear energy loss dominates. A nice example is illustrated in Figure 27 (Eriksson et al., 1967). The oscillatory dependence of the electronic stopping cross section, S_e, on Z_1 stems from the so-called Ramsauer–Townsend effect. The cross section for electron scattering on the penetrating ion may be written as a sum over angular momenta and at low velocity the s-wave cross section dominates. With increasing strength of the scattering potential, the s-wave phase shift increases, and the cross

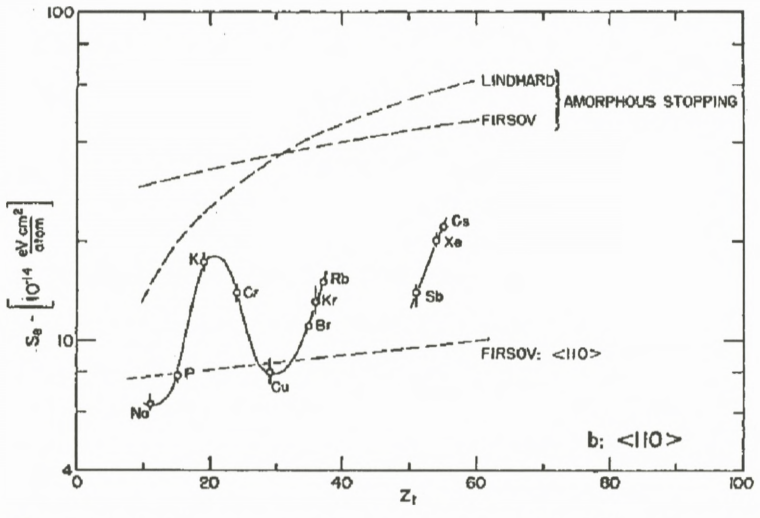

Figure 27. Electronic-stopping cross section at velocity $v = 1.5 \times 10^8$ cm/s *versus* the atomic number of the projectile, derived from the range of a perfectly channeled ion along a ⟨110⟩ direction in tungsten (Eriksson et al., 1967).

section has strong minima when the phase shift passes through multiples of π (Finnemann, 1968; Briggs and Pathak, 1973). The oscillations were first seen in the stopping in amorphous foils but the elimination of atomic recoils and the confinement of electronic scattering to the thin electron gas far from atoms make the oscillations much more prominent.

At high velocities the slowing down is mainly due to electronic energy loss. For small Z_1 it may be obtained by a quantum perturbation calculation. The resulting Bethe–Bloch formula may be written as an integral over impact parameters, leading to a logarithm of the ratio of an adiabatic radius divided by half the reduced wavelength of the electrons in the ion rest frame,

$$-\frac{\mathrm{d}E}{\mathrm{d}x} = NS_e = \frac{4\pi Z_1^2 e^4}{mv^2} NZ_2 \ln \frac{v/\omega}{\lambda/2}. \tag{18}$$

The observations of a reduced electronic energy loss for a substantial fraction of MeV protons penetrating several micron thick crystals demonstrated convincingly that channeling is not a simple transparency effect for low energy ions.

Asymptotically for large v the expression in Equation (18) has equal contributions from large and small impact parameters (equipartition). Therefore the energy loss is at high velocities reduced by about a factor of two for the best channeled particles (Lindhard, 1965). As demonstrated by Esbensen and Golovchenko

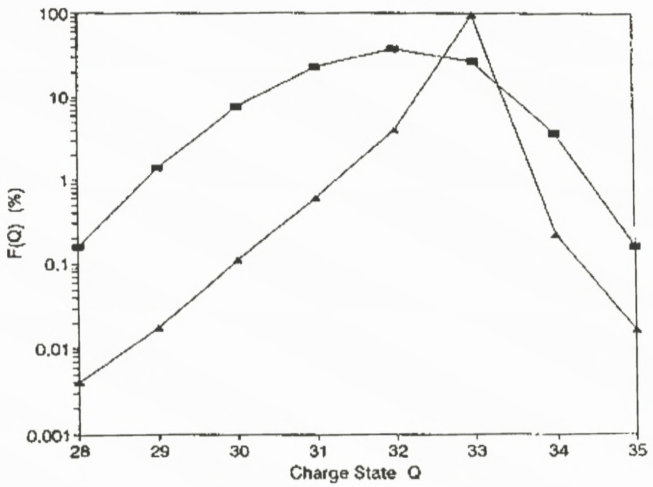

Figure 28. Charge-state distributions for a random (□) and a ⟨110⟩ aligned (Δ) beam of 15.3 MeV/u Br^{33+} ions after passage of a 1 μm Si crystal (Andersen et al., 1996).

(1976), the theory simplifies in the high-velocity limit, and excellent agreement with measurements of the energy loss for relativistic channeled particles in thin Si and Ge crystals was obtained (Esbensen et al., 1978). Also the shape of the energy distribution for channeled particles could be accounted for when fluctuations of large energy transfers in single collisions with electrons were taken into account (Landau distribution).

Many other experiments and calculations on the stopping of channeled ions have been published (Cohen and Dauvergne, 2004) but still the full potential of such studies for testing the stopping power theory has in my view not been realised. An attempt at a detailed comparison with standard stopping theory for swift heavy ions is discussed in the following.

In the experiment 15.3 MeV/u Br^{33+} ions were passed through a very thin Si crystal and both the emergent charge state and the energy-loss spectrum were measured with a magnetic spectrometer (Andersen et al., 1996). As illustrated in Figure 28, the 33+ ions with only the K-shell electrons remaining undergo very little capture or loss of electrons when the ions are incident along a ⟨110⟩ axis. This phenomenon of "frozen charge state" was especially investigated and applied by Datz and co-workers in Oak Ridge in their pioneering experiments on channeling of high-energy, heavy ions (Gemmell, 1974; Krause and Datz, 1996). It is important for the analysis of the energy loss because the complication of a fluctuating charge state is removed.

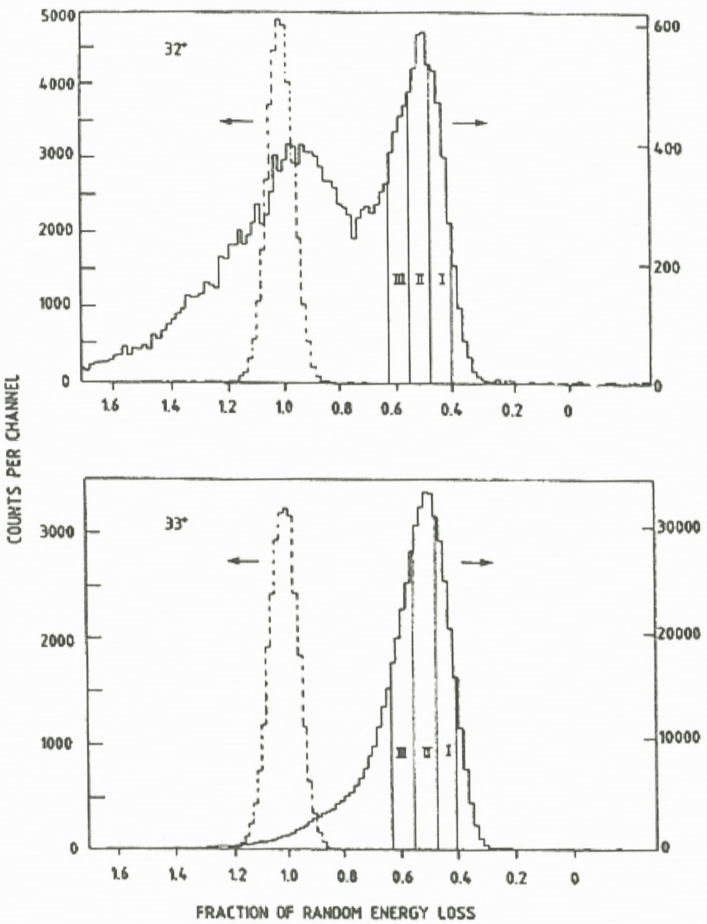

Figure 29. Energy-loss of transmitted 32+ and 33+ ions for a beam of 15.6 MeV/u $^{79}Br^{33+}$ ions. Spectra for random (- - - -) and ⟨110⟩ (—) alignment are shown as functions of the energy loss relative to the average random loss of $\Delta E = 4.9$ MeV for the 1 μm thick Si target (Andersen et al., 1996).

The energy spectra for exiting 33+ and 32+ ions are shown in Figure 29. For reference, also the energy spectrum for ions incident in a random (i.e., non-channeling) direction is shown, and the energy loss is given as a fraction of the random energy loss (4.9 MeV for 1μm Si). Nearly all the 33+ ions have an energy loss much smaller than for random incidence, reflecting that nearly all the ions are channeled. The spectrum for the much fewer 32+ ions contains two parts, well channeled ions which have captured a valence electron, with an energy spectrum

similar to that for 33+ ions, and poorly channeled ions which have entered the crystal close to a string and scattered to angles of order ψ_1, with energy loss similar to or even larger than random. There is also a small component of such ions in the 33+ spectrum but it is strongly enhanced for 32+ ions because the capture probability is much higher for random than for channeled ions (Figure 28).

For the analysis of the energy loss, the well channeled ions have been divided into three groups. For fixed trajectory, the straggling in energy loss is small. This can be seen from the width of the random energy loss peak which has about equal contributions from charge-exchange straggling and Bohr straggling (fluctuations in hard collisions). For channeled particles there is only the Bohr straggling and it is reduced due to the lower electron density. In contrast to the situation for relativistic particles discussed above, the width of the energy loss distribution therefore comes mainly from the distribution in transverse energy and the associated variation of the allowed area in the transverse plane. If the spatial variation of the energy loss rate is known, the energy distribution can be calculated and compared with the measurement.

The analysis was based on a simple description of the energy loss as consisting of three parts, the energy transfers to K-, L-, and M-shell electrons. The corresponding oscillator strengths and excitation frequencies could be estimated rather accurately, and the dependence of the energy loss on transverse energy was then calculated. Compared with the Bethe–Bloch formula given above there are two important corrections for heavy ions. First Bohr's kappa (Equation (12) with $Z_2 = 1$) is larger than unity and the classical counterpart, the Bohr formula, should be applied instead, with the reduced electron wavelength replaced by the classical collision diameter. Second, there may be a significant so-called Barkas correction which is of third order in Z_1. It is about 5%, only, for the present case. Good agreement with the measurement was obtained. The dependence of the stopping on transverse energy turns out to come partly from the spatial variation of the density of valence (M-shell) electrons, partly from the adiabatic cut-off of energy loss to the L-shell at large impact parameters with atoms.

18. Crystal as Special Target for Atomic Processes

Studies of energy loss are just one example of the use of crystals as special targets for measurements on atomic processes (Krause and Datz, 1996). For channeled ions, the target is essentially a gas of the valence electrons. This has been utilised to study capture processes like radiative electron capture and dielectronic electron capture.

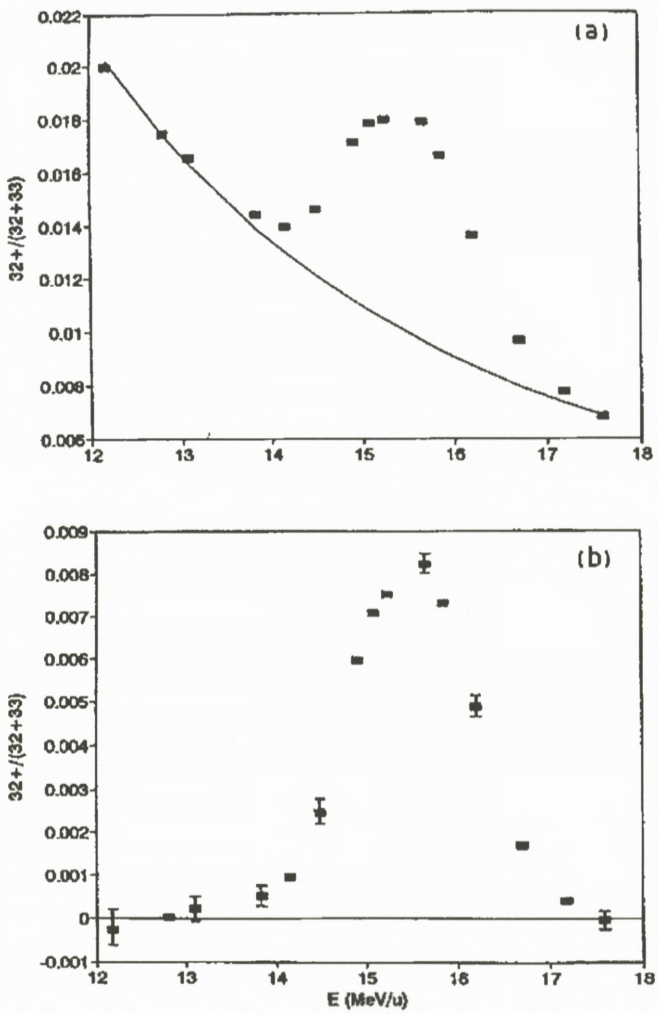

Figure 30. (a) The charge state fraction $32^+/(32^+ + 33^+)$ for channeled ions with energy loss in the windows I, II, and III in Figure 29, as a function of the ion energy. (b) Data in (a) after subtraction of a smooth background (Andersen et al., 1996).

An example, from the experiment with Br^{33+} ions discussed above, is illustrated in Figure 30. The ratio between the numbers of 32+ and 33+ ions within the energy window I+II+III in Figure 29 is here plotted as a function of the bombarding energy. The peak in Figure 30b, obtained after subtraction of a smooth background from other capture processes, occurs at a velocity where the energy

of a valence electron in the ion frame of reference matches the K-shell binding energy minus twice the L-shell binding. An electron can then be captured with simultaneous excitation of a K-shell electron. The width of the resonance comes from the spread of electron velocities in the electron gas.

Another process which should be mentioned in this connection is resonant coherent excitation, sometimes called the Okorokov effect (Okorokov, 1965). Here a Fourier component of the periodic field from a string of atoms is used to excite a bound electron. Channeling is again used to avoid close collisions and thereby to maintain a well defined atomic state during the interaction. The excitation can be observed either by detection of radiative de-excitation outside the crystal or by observation of the emergent charge state distribution as a function of bombarding energy. At velocities where a multiple of the frequency of collisions with atoms on a string matches a transition frequency in the ion, the atomic excitation gives rise to an increase in the rate of electron loss and hence to an increase in the charge state. The effect was first observed unambiguously at Oak Ridge (Moak et al., 1979). Recently, mainly a Japanese group working at the high-energy accelerator laboratory RIKEN has been active in this area, extending the observations to heavier ions carrying a few electrons (Nakai et al., 2005).

19. Concluding Remarks

The physics of channeling is rich in interesting, sometimes quite surprising phenomena, and channeling and blocking have very many applications. I have reviewed some of the aspects of channeling which I have found it most exciting to work on and hope that the reader will experience some of this excitement. With the rapid development of computers, simulation has become increasingly important in the interpretation of experiments, but the analytical theory founded by Jens Lindhard remains the basis for our understanding of the phenomena.

Channeling is a mature field but there are still challenging problems. The basic binary scattering is described by a screened Coulomb potential and, except for simple, limiting cases, there is considerable uncertainty in the representation of the combined screening by target and projectile electrons. I have mentioned two cases where this uncertainty is a problem. One is the application of blocking to measure nuclear lifetimes. It is important to be able to compare blocking dips for reaction products and for elastically scattered projectile ions, and this requires an accurate scaling of the critical angle for blocking with the atomic number of the blocked ions. Another example is the analysis of "heating" and "cooling" phenomena in the penetration of energetic heavy ions through thin crystals where

a precise description of the dependence of the interaction potential on the ion charge state is needed.

Channeling of ions in crystals makes it possible to study the impact parameter dependence of atomic processes. The simplest example is energy loss, and studies of the modified stopping under channeling conditions played an important role in the discovery of channeling. Usually the question has been what we can learn about ion channeling from the energy loss spectrum. One may turn the question around and ask what we have learned about energy loss processes from channeling observations and what we can still learn. I have argued that if experiments and calculations are planned with this question in mind there may be scope for new investigations of the energy loss of channeled ions. New opportunities are also offered by the recently discovered "cooling" and "heating" phenomena which are very sensitive to the impact parameter dependence of the capture and loss of electrons.

References

Alguard M.J., Swent R.L., Pantell R.H., Datz S., Barrett J.H., Berman B.L. and Bloom S.D. (1980): Radiation from channeled leptons. Nucl Instrum Methods **170**, 7–13

Andersen J.U. and Feldman L.C. (1970): Comparison of average-potential models and binary-collision models of axial channeling and blocking. Phys Rev B **1**, 2063–2069

Andersen J.U. and Lægsgaard E. (1980): Characteristic radiation from channeled electrons. Phys Rev Lett **44**, 1979–1982

Andersen J.U. and Uguzzoni A. (1990): A restricted equilibrium in phase space for axial channeling. Nucl Instrum Methods Phys Res B **48**, 181–186

Andersen J.U., Lægsgaard E., Nielsen K.O., Gibson W.M., Forster J.S., Mitchell I.V. and Ward D. (1976): Time evolution of heavy-ion-induced fission studied by crystal blocking. Phys Rev Lett **36**, 1539–1542

Andersen J.U., Andersen S.K. and Augustyniak W.M. (1977): Channeling of electrons and positrons. Kgl Dan Vid Selsk Mat Fys Medd **39, no. 10**, 1–58

Andersen J.U., Jensen A.S., Jørgensen K., Lægsgaard E., Nielsen K.O., Forster J.S., Mitchell I.V., Ward D., Gibson W.M. and Cuomo J.J. (1980): Lifetime measurements for heavy-ion-induced fission by the crystal-blocking technique. Kgl Dan Vid Selsk Mat Fys Medd **40, no. 7**, 1–56

Andersen J.U., Bonderup E., Lægsgaard E., Marsh B.B. and Sørensen A.H. (1982): Axial channeling radiation from MeV electrons. Nucl Instrum Methods **194**, 209–224

Andersen J.U., Bonderup E. and Pantell R.H. (1983a): Channeling radiation. Ann Rev Nucl Part Sci **33**, 453–504

Andersen J.U., Bonderup E., Lægsgaard E. and Sørensen A.H. (1983b): Incoherent scattering of electrons and linewidth of planar-channeling radiation. Physica Scripta **28**, 308–330

Andersen J.U., Chevallier J., Ball G.C., Davies W.G., Forster J.S., Geiger J.S., Davies J.A., Geissel H. and Kanter E.P. (1996): Dielectronic recombination and energy loss for He-like ^{79}Br ions channeled in a thin single crystal of Si. Phys Rev A **54**, 624–635

Assmann W., Huber H., Karamian S.A., Grüner F., Mieskes H.D., Andersen J.U., Posselt M. and Schmidt B. (1999): Transverse cooling or heating of channeled ions by electron capture and loss. Phys Rev Lett **83**, 1759–1762

Barrett J.H. (1973a): Monte Carlo channeling calculations. Phys Rev B **3**, 1527–1547

Barrett J.H. (1973b): Breakdown of the statistical-equilibrium hypothesis in channeling. Phys Rev Lett **31**, 1542–1545

Baurichter A., Biino C., Clément M., Doble N., Elsener K., Fidecaro G., Freund A., Gatignon L., Grafström P., Gyr M., Hage-Ali M., Herr W., Keppler P., Kirsebom K., Klem J., Major J., Medenwaldt R., Mikkelsen U., Møller S.P., Siffert P., Uggerhøj E., Vilakazi Z.Z. and Weisse E. (2000): Channeling of high-energy particles in bent crystals – Experiments at the CERN SPS. Nucl Instrum Methods in Phys Res B **164–165**, 27–43

Bech Nielsen B., Andersen J.U. and Pearton S.J. (1988): Lattice location of deuterium interacting with the boron acceptor in silicon. Phys Rev Lett **60**, 321–324

Beloshitsky V.V., Kumakhov M.A. and Muralev V.A. (1972): Multiple scattering of channeled ions in crystals. Rad Effects **13**, 9–22

Berg Rasmussen F. and Bech Nielsen B. (1994): Microstructure of the nitrogen pair in crystalline silicon studied by ion channeling. Phys Rev B **49**, 16353–16360

Bonderup E., Esbensen H., Andersen J.U. and Schiøtt H.E. (1972): Calculations on axial dechanneling. Rad Effects **12**, 261–266

Briggs J.C. and Pathak A.P. (1973): Momentum transfer cross sections and the Z1 oscillations in stopping power. J Phys C **6**, L153–L157

Cohen C. and Dauvergne D. (2004): High energy ion channeling; Principles and typical applications. Nucl Instrum Methods Phys Res B **225**, 40–71

Datz S., Martin F.W., Moak C.D., Appleton B.R. and Bridwell L.B. (1972): Charge changing collisions of channeled oxygen ions in gold. Rad Effects **12**, 163–169

Datz S., Berman B.L., Dahling B.A., Hynes M.V., Park H., Kephart J.O., Klein R.K. and Pantell R.H. (1986): On the dependence of electron planar channeling radiation upon lattice vibration amplitude. Nucl Instrum Methods Phys Res B **13**, 19–22

Davies J.D. (1983): The channeling phenomenon – And some of its applications. Physica Scripta **28**, 294–302

Domeij B. and Björkqvist K. (1965): Anisotropic emission of α-particles from a monocrystalline source. Phys Lett **14**, 127–128

Drouart A., Charvet J.L., Dayras R., Nalpas L., Volant C., Chbihi A., Escano Rodriguez C., Frankland J.D., Morjean M., Chevallier M., Dauvergne D., Kirsch R., Lautesse P., Ray C., Testa E., Cohen C., L'Hoir A., Jacquet D. and Laget M. (2005): Evidence of $Z = 120$ compound nucleus formation from lifetime measurements in the ^{238}U+Ni reaction at 6.62 MeV/nucleon. In: Proceedings of International Symposium on Exotic Nuclei, Peterhof 2004. World Scientific, Singapore, pp 192–197

Eriksson L., Davies J.A. and Jespersgaard P. (1967): Range measurements in oriented tungsten single crystals (0.1–1.0 MeV). I. Electronic and nuclear stopping powers. Phys Rev **161**, 219–234

Esbensen H. and Golovchenko J.A. (1976): Energy loss of fast channeled particles. Nucl Phys A **298**, 382–396

Esbensen H., Fich O., Golovchenko J.A., Madsen S., Nielsen H., Schiøtt H.E., Uggerhøj E., Vraast-Thomsen C., Charpak G., Majewski S., Odyniec G., Petersen G., Sauli F., Ponpon J.P. and

Siffert P. (1978): Random and channeled energy loss in thin germanium and silicon crystals for positive and negative 2–15-GeV/c pions, kaons, and protons. Phys Rev B **18**, 1039–1054

Feldman L.C., Mayer J.W. and Picraux S.T. (1982): Materials Analysis by Ion Channeling. Academic Press, New York

Finnemann J. (1968): En redegørelse for resultaterne af beregninger over spredning af elektroner med lav energi på afskærmede Coulombfelter. Thesis under supervision of J. Lindhard, Physics Institute, University of Aarhus

Forster J.S., Andersen J.U., Beene J.R., Broude C., Chevallier J., Galindo-Uribarri A., Gomez del Campo J., Karamian S.A., Krause H.F., Radford D., Uguzzoni A. and Vane C.R. (2006): to be published

Gärtner K., Hehl K. and Schlotzhauer G. (1984): Axial dechanneling: II. Point defects. Nucl Instrum Methods B **4**, 55–62

Gemmell D.S. (1974): Channeling and related effects in the motion of charged particles through crystals. Rev Mod Phys **46**, 129–227

Gibson W.M. (1975): Blocking measurements of nuclear decay times. Ann Rev Nucl Sci **25**, 465–508

Grüner F., Assmann W., Bell F., Schubert M., Andersen J.U., Karamian S., Bergmaier A., Dollinger G., Görgens L., Günther W. and Toulemonde M. (2003): Transverse cooling and heating in ion channeling. Phys Rev B **68**, 174104-1 to 12

Guanere M., Sillou D., Spighel M., Cue N., Gaillard M.J., Kirsch R.G., Poizat J.-C., Remmillieux J., Berman B.L., Cattillon P., Roussel L. and Temmer G.M. (1982): Sharp-line and broad-continuum radiation from electrons channeled in diamond. Nucl Instrum Methods **194**, 225–228

Hau L.V. and Andersen J.U. (1993a): Channeling radiation beyond the continuum model: The phonon "Lamb shift" and higher-order corrections. Phys Rev A **47**, 4007–4032

Hau L.V. and Andersen J.U. (1993b): Line shifts of channeling radiation from MeV electrons. Rad Eff Def Sol **25**, 75–80

Hau L.V., Lægsgaard E. and Andersen J.U. (1990): Thermal vibrations in Si studied by channeling-radiation spectroscopy. Nucl Instrum Methods Phys Res B **48**, 244–247

Hofsäss H. (1996): Emission channeling. Hyperfine Interactions **97-8**, 247–283

Karamian S.A., Forster J.S., Andersen J.U., Assmann W., Broude C., Chevallier J., Geiger J.S., Grüner F., Khodyrev V.A., Malaguti F. and Uguzzoni A. (2003): Fission lifetimes of Th nuclei measured by crystal blocking. Eur Phys J A **17**, 49–56

Kennedy E.F., Bech Nielsen B. and Andersen J.U. (1992): Planar channeling dips in backscattering yield. Nucl Instrum Methods in Phys Res B **67**, 236–240

Krause H.F. and Datz S. (1996): Channeling heavy ions through crystalline lattices. Adv At Mol Opt Phys **37**, 139–180

Kumakhov M.A. (1976): On the theory of electromagnetic radiation of charged particles in a crystal. Phys Lett A **57**, 17–18

Lervig Ph., Lindhard J. and Nielsen V. (1967): Quantal treatment of directional effects for energetic charged particles in crystal lattices. Nucl Phys A **96**, 481–504

Lindhard J. (1965): Influence of crystal lattice on motion of energetic charged particles. Kgl Dan Vid Selsk Mat Fys Medd **34, no. 14**, 1–64

Lindhard J. and Nielsen V. (1971): Studies in statistical dynamics. Kgl Dan Vid Selsk Mat Fys Medd **38, no. 9**, 1–42

Malyshevsky V.S. (2005): Statistical theory of charge state distributions of channeled heavy ions. Phys Rev B **72**, 094109-1 to 10

Mayer J.W., Eriksson L. and Davies J.A. (1970): Ion Implantation in Semiconductors. Academic Press, New York

Moak C.D., Datz S., Crawford O.H., Krause H.F., Dittner P.F., Gomez del Campo J., Biggerstaff J.A., Miller P.D., Hvelplund P. and Knudsen H. (1979): Resonant coherent excitation of channeled ions. Phys Rev A **19**, 977–993

Nakai Y., Ikeda T., Kanai Y., Kambara T., Fukinishi N., Komaki K., Kondo C., Azuma T. and Yamazaki Y. (2005): Resonant coherent excitation of 2s electron of Li-like Fe ions to the $n = 3$ states. Nucl Instrum Methods Phys Res B **230**, 90–95

Okorokov V.V. (1965): The coherent excitation of nuclei moving through a crystal. Yad Fiz **2**, 1009 [Sov J Nucl Phys **2**, 719 (1966)]

Oshiyama T. and Mannami M. (1981): Diffusion models of dechanneling of energetic H^+-ions in single crystals. Phys Lett **81A**, 43–46

Pedersen M.J., Andersen J.U. and Augustyniak W.M. (1972): Channeling of positrons. Rad Effects **12**, 47–52

Sørensen A.H. and Uggerhøj E. (1987): Channeling and channeling radiation. Nature **325**, 311–318

Sørensen A.H. and Uggerhøj E. (1989): Channeling, radiation and applications. Nucl Sci Appl **3**, 147–205

Tulinov A.F., Kulikauskas V.S. and Malov M.M. (1965): Proton scattering from a tungsten single crystal. Phys Lett **18**, 304–307

Uggerhøj E. (1966): Orientation dependence of the emission of positrons and electrons from ^{64}Cu embedded in single crystals. Phys Lett **22**, 382–383

Uggerhøj E. and Andersen J.U. (1968): Influence of lattice structure on motion of positrons and electrons through single crystals. Can J Phys **46**, 543–550

Uggerhøj U.I. (2005): The interaction of relativistic particles with strong crystalline fields. Rev Mod Phys **77**, 1131–1171

Uguzzoni A., Gärtner K., Lulli G. and Andersen J.U. (2000): The minimum yield in channeling. Nucl Instrum Methods B **164–165**, 53–60